

DEVELOPMENT OF RIKEN 28 GHz SC-ECRISs FOR SYNTHESIZING SUPER-HEAVY ELEMENTS

T. Nagatomo[†], Y. Higurashi, J. Ohnishi, A. Uchiyama, M. Fujimaki, K. Kumagai, N. Fukunishi, N. Sakamoto, T. Nakagawa, and O. Kamigaito, Nishina Center for Accelerator-based Science, RIKEN, Wako, Saitama 351-0198, Japan

Abstract

Production of intense metallic ion beams were required at RIKEN to synthesize new elements with atomic numbers higher than 118. To meet this requirement, we systematically studied the optimization of RIKEN 28 GHz SC-ECRIS performance. Using these results, we produced V^{13+} ion beam of 400 μA at ~ 2 kW microwave power (18+28 GHz) and a B_{ext} (maximum magnetic mirror field at the beam extraction side) of 1.4 T. For long-term operation, we successfully produced an intense and stable beam (100–200 μA). To progress this project, new super-conducting RF cavities are now under construction downstream of the RIKEN heavy-ion linac (RILAC) to increase beam energy. In this project, we also constructed a new 28 GHz SC-ECRIS based on these results to increase beam intensities. In addition, three sets of movable slits were installed in the low energy beam transport (LEBT) to inject the high-quality beam into the upgraded RIKEN heavy-ion LINAC (RILAC) to control the size of the transverse emittance of the beam.

INTRODUCTION

After synthesizing a super-heavy element (with an atomic number of 113), a new project was started at RIKEN for synthesizing a new element with an atomic number higher than 118 [1, 2]. For this project, intense, highly charged metallic ion beams, using ions such as Titanium (Ti^{13+}), Vanadium (V^{13+}), and Chromium (Cr^{13+}), were required. To progress the project, the RIKEN heavy-ion linac (RILAC) is up-graded by adding new super-conducting ratio frequency (RF) cavities. In this project, we also constructed a new SC-ECRIS for increasing beam intensity.

The up-graded RILAC is also used as an injector accelerator for the RIKEN radioactive isotope beam (RIBF) project [2, 3]. To accelerate the heavy ion beam for RIBF, the ion source has to provide it with a mass to charge state ratio smaller than three (e.g., $^{48}Ca^{16+}$ and $^{70}Zn^{24+}$). High electron density (n_e) and long confinement time (τ_i) in the ion source plasma are required to produce these highly charged, heavy ions. Using a crude calculation [4], the required $n_e \tau_i$ for $^{48}Ca^{16+}$ ion production was in the order of 10^9 (sec/cm³), which is one order of magnitude larger than the required $n_e \tau_i$ for the $^{51}V^{13+}$ ion (in the order of 10^8 (sec/cm³)). Therefore, it was necessary to design an ion source that could provide the optimum condition to cover a wide range of $n_e \tau_i$ in the ion source plasma.

In the last three decades, two guidelines (scaling laws [4, 5] and high B mode [6-8]) have been proposed and used to design and develop ion sources. Scaling laws were proposed to describe the effects of the main ion source parameters (microwave power, magnetic field strength, microwave frequency, mass of heavy ions, etc.) on the output beam of highly charged heavy ions. These studies reported that the strength of the magnetic mirror affects the optimum charge state (i.e., a higher mirror ratio yields higher output ion beam charge states). In the middle of the 1990s, the high-B mode, which employs a high magnetic mirror ratio to confine the plasma, was proposed to increase the beam intensities of highly charged heavy ions. To meet the requirement for the project, we systematically studied the effects of a magnetic mirror on beam intensity based on these guidelines.

It was clear that we need to produce enough metallic vapor to produce an intense beam. In addition, high transmission efficiency in the low-energy beam transport line (LEBT) was required for efficient operation of the ion source. Considering these points, we constructed and developed an ion source, a high temperature oven (HTO), and a LEBT for this project.

In the second and third sections of this contribution, the results of optimization of the ion source performance and the metallic ion beam production with HTO are described. In the fourth section, we present the structure of the LEBT and the first results from the new ion source.

OPTIMIZATION OF THE MAGNETIC MIRROR

In the test experiments for magnetic mirror effects, we used two different types of ion sources, Liquid-He-free SC-ECRIS [9] and RIKEN 28 GHz SC-ECRIS [10]. The RIKEN 28 GHz SC-ECRIS has six solenoid coils to produce a flexible mirror magnetic field in the axial direction, and it can produce both classical and flat B_{min} [11].

Generally, as an ECRIS has three magnetic mirrors (B_{inj}/B_{min} , B_r/B_{min} , and B_{ext}/B_{min}) (B_{inj} , maximum magnetic mirror field at the microwave injection side; B_{ext} , maximum magnetic mirror field at the beam extraction side; B_r , the radial magnetic field; and B_{min} , minimum strength of the mirror magnetic field), various combinations of the magnetic mirrors can exist to produce a beam of highly charged heavy ions. Therefore, we needed to carefully study the effects of the magnetic mirror to maximize beam intensity. Figure 1 a) and b) show the normalized beam intensities as a function of B_{inj}/B_{ext} and B_r/B_{ext} with the RIKEN 28 GHz SC-ECRIS (18 and 28 GHz microwaves) and the Liquid-He-free SC-ECRIS (18 GHz microwaves).

[†]nagatomo@riken.jp

Content from this work may be used under the terms of the CC BY 3.0 licence (© 2018). Any distribution of this work must maintain attribution to the author(s), title of the work, publisher, and DOI.

The beam intensity of various charge state heavy ions produced with our ECRISs appeared saturated at $B_r=1-1.2B_{ext}$ and $B_{inj}=1.6-2.0B_{ext}$. The results of RIKEN 28 GHz SC-ECRIS appear similar to the results from the Liquid-He free SC-ECRIS. These results are well-reproduced with high B mode operation (B_{inj}/B_{ext} was ~ 2.0 and B_r/B_{ext} was ~ 1.0) [8].

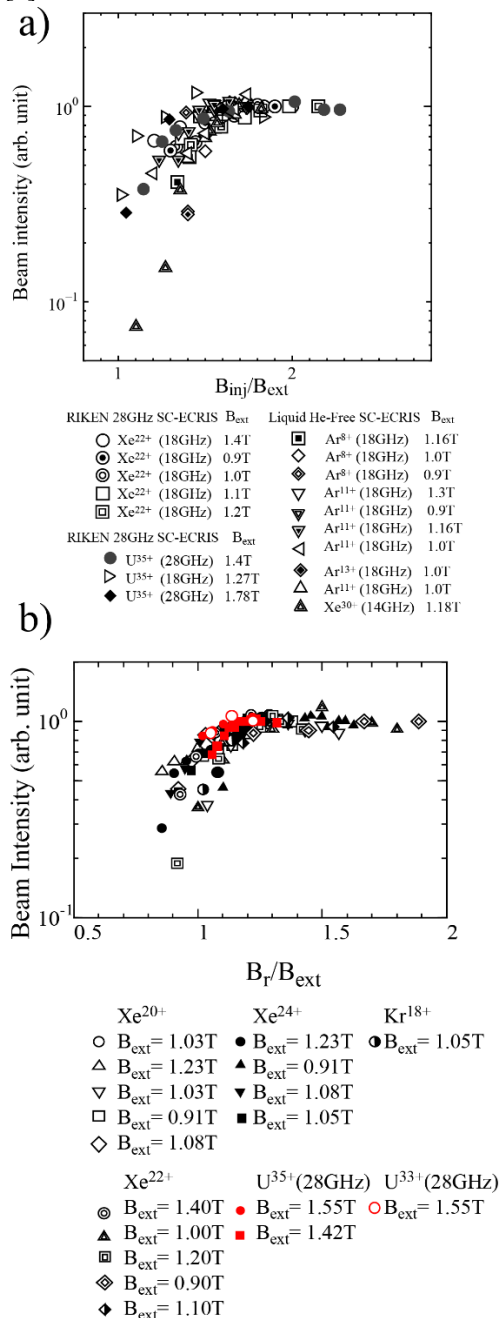


Figure 1: a) Beam intensity of highly charged heavy ions as a function of B_{inj}/B_{ext} and b) beam intensity of highly charged heavy ions as a function of B_r/B_{ext} .

To study the relationship between B_{ext} and B_{inj} (or B_r) in more detail, we provided two-dimensional contour maps (B_r vs. B_{ext} and B_{inj} vs. B_{ext}) for the beam intensity of Xe²²⁺ produced with the RIKEN 28 GHz SC-ECRIS (18 GHz

microwaves injection) (Fig. 2 a) and b)). In these figures, red and blue colors indicate the highest and lowest beam intensities, respectively. B_{min} was set to ~ 0.5 T, which is the optimum strength for maximizing the beam intensity with 18 GHz microwave injection. The extraction voltage and the microwave power were 21 kV and ~ 500 W, respectively. The gas pressure and biased disc condition (negative voltage and position) were changed slightly to maximize beam intensity at the measurement points. In this experiment, we observed that the gas pressure for maximizing beam intensity increased with increasing magnetic field strength. Beam intensity increased with increasing both B_r (or B_{inj}) and B_{ext} , and it became constant above a certain value of magnetic field strength (Fig. 2). To maximize beam intensity, B_r and B_{ext} were ~ 1.5 and ~ 1.2 T, respectively (Fig. 1 a)). The corresponding B_{inj} and B_{ext} values were ~ 2.2 and ~ 1.2 T, respectively (Fig. 1 b)).

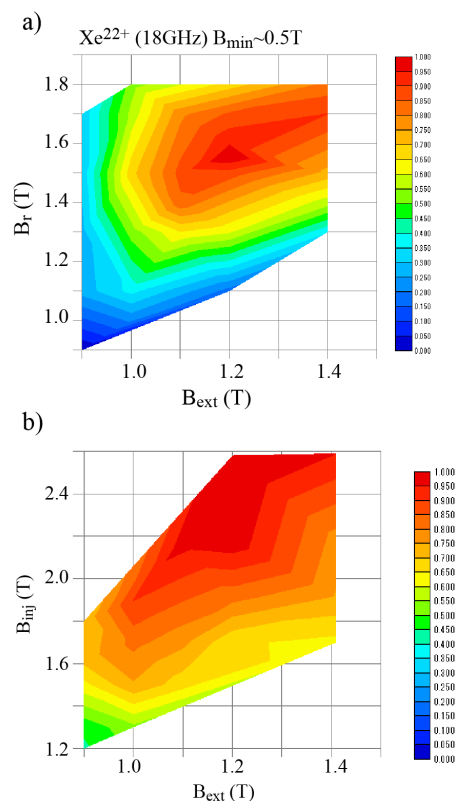


Figure 2: Two-dimensional contour maps (a) B_r vs. B_{ext} and b) B_{inj} vs. B_{ext} for the Xe²²⁺ ion beam.

To investigate the effect of B_{ext} on beam intensity, we measured the optimum B_{ext} for various charge states of Ar and Xe ions with 18 and 28 GHz in the same procedures shown in Fig. 2. As the beam intensity was gradually changed as a function of magnetic field strength, it was difficult to accurately determine the B_{ext} causing beam intensity saturation. Therefore, we chose, as a reference, a B_{ext} that provided ~ 95 % of the maximum beam intensity. We observed that B_{ext} , which provided ~ 95 % of the maximum value (optimum B_{ext}) for highly charged Xe ions, increased from ~ 1.2 to ~ 1.6 T when the charge state increased from

22 to 30. We also observed the same tendency for the highly charged Ar ions with the Liquid-He-free SC-ECRIS. The optimum B_{ext} increased from ~ 1.1 to ~ 1.25 T when the charge state increased from 8 to 13 for the Ar ions.

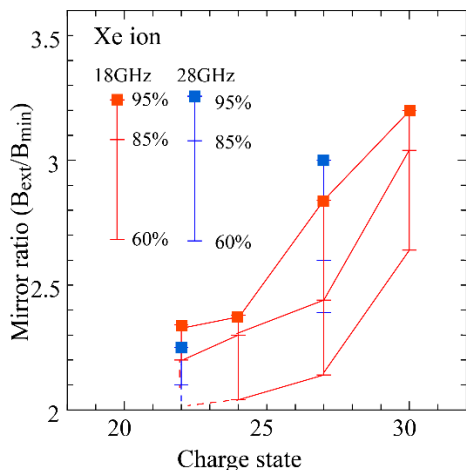


Figure 3: Magnetic mirror ratio ($B_{\text{ext}}/B_{\text{min}}$) as a function of the charge state for Xe ions with 18 and 28 GHz microwaves.

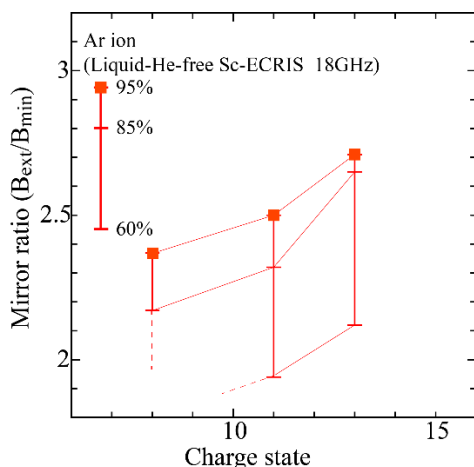


Figure 4: Magnetic mirror ratio ($B_{\text{ext}}/B_{\text{min}}$) as a function of the charge state for Ar ions.

As described in refs. [4, 5], the optimum charge state depends on the mirror ratio when B_{min} is fixed. Figure 3 and 4 show the mirror ratio ($B_{\text{ext}}/B_{\text{min}}$) that provides $\sim 95\%$ of the maximum beam intensity as a function of the charge state of Xe and Ar ions. The results for Xe and Ar ions were obtained from the two-dimensional contour maps (B_r vs. B_{ext} and B_{inj} vs. B_{ext} , respectively). $\sim 85\%$ and $\sim 60\%$ of the maximum beam intensity were also plotted in these figures as a reference. The mirror ratio for the optimum B_{ext} increased from ~ 2.2 to ~ 3.2 with increases in the charge state of the Xe ions. We observed the same tendency for the Liquid-He-free SC-ECRIS when the mirror ratio increased from ~ 2.3 to ~ 2.7 when the charge state increased from 8 to 13. These results were qualitatively reproduced by the scaling law. These experimental results were obtained for a low microwave power density (below several 100 W/L).

We might observe a different tendency at a higher RF power (i.e., 1 kW/L).

METALLIC ION BEAM PRODUCTION

As mentioned in the introduction, since the $n_e \tau_i$ for V^{13+} ions is in the order of 10^8 (sec/cm³), it is assumed that the V^{13+} ions are in the same region ($n_e \tau_i$) as the Xe^{24-27+} ions. As described in ref. [4, 12, 13, 14], $n_e \tau_i$ depends on the mirror ratio. Therefore, from the results shown in Fig. 3, the magnetic mirror ratio ($B_{\text{ext}}/B_{\text{min}}$) for the V^{13+} ions was assumed to be 2.2–2.7. If we chose a B_{min} of 0.6 T for 28 GHz, which is the optimum value for maximizing the beam intensity, the optimum B_{ext} might be 1.3–1.6 T. In the test experiment, we observed that the beam intensity decreased slightly when B_{ext} decreased from 1.6 to 1.4 T. On the bases of these results, we chose $B_{\text{ext}}=1.4$ T in this test experiment.

For production of the vapor, we used the HTO [15]. For long-term operation, we fabricated a new crucible, which had approximately twice the volume of the old crucible [16]. To obtain a sufficient temperature for evaporating the materials, a detailed simulation was carefully performed, and a sufficiently high temperature was obtained to produce the vapor. The detailed results are presented in ref. [15]. Enough metallic vapor should be provided to maximize beam intensity. To optimize the vapor pressure, we measured the beam intensity as a function of oven power at a fixed microwave power, as shown in Fig. 5. The beam intensity increased with increasing oven power and it seems that the intensity was saturated at the highest oven power. We used the same procedure at each microwave power.

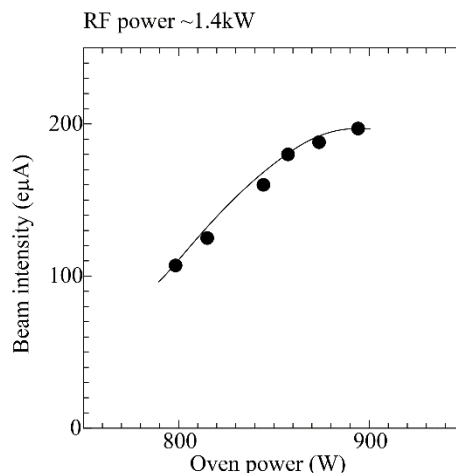


Figure 5: Beam intensity of the V^{13+} ions as a function of oven power at a microwave power of ~ 1.4 kW.

Figure 6 shows that beam intensity and X-ray heat load as a function of microwave power for $B_{\text{ext}} = 1.4$ T. We used the double frequencies injection (18 GHz (maximum power of several 100 W) + 28 GHz) [17] for producing the stable beam. Both the beam intensity and heat load increased with increasing microwave power. At ~ 2 kW we obtained 400 eµA of V^{13+} ions, and the X-ray heat load was ~ 1.2 W, which was sufficiently low for safe operation of

Content from this work may be used under the terms of the CC BY 3.0 licence (© 2018). Any distribution of this work must maintain attribution to the author(s), title of the work, publisher, and DOI.

the ion source. Figure 7 shows the oven power required to maximize beam intensity at each microwave power. The oven power increased linearly with increasing microwave power. The consumption rate of the material was ~ 2.4 mg/h for lower microwave power (~ 1.2 kW), which was sufficiently low to operate the ion source for a long time.

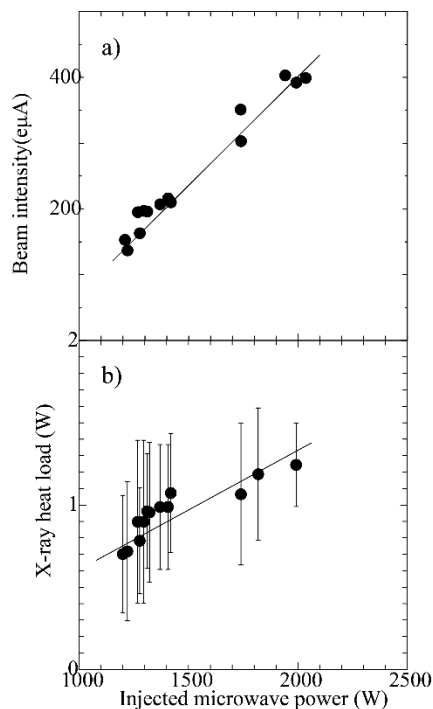


Figure 6: a) Beam intensity of the V^{13+} ions as a function of microwave power and b) X-ray heat load in the cryostat as a function of microwave power.

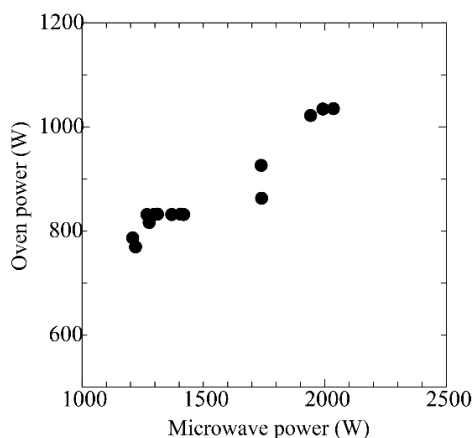


Figure 7: Optimum oven power as a function of microwave power.

For long-term operation, we successfully produced an intense beam (100–200 eμA) of V^{13+} ions. However, we wanted to improve the HTO's performance at higher material consumption for long-term operation, as described in ref. [15].

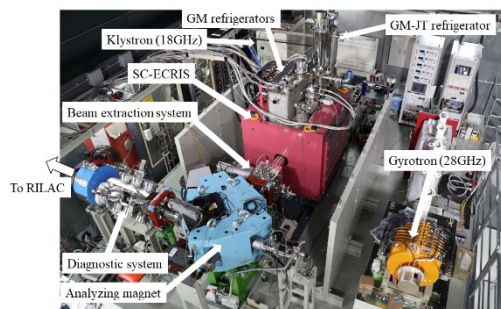


Figure 8: Photograph of the 28 GHz SC-ECRIS.

NEW ION SOURCE AND LEBT

As mentioned in the introduction, the ion source was required to provide a plasma condition of $n_e \tau_i \sim 10^9$ (sec/cm³) to produce Ca^{16+} ions, which is the same order magnitude of $n_e \tau_i$ for Xe^{30+} . To meet this requirement, the mirror ratio (B_{ext}/B_{min}) should be greater than 3. If we chose $B_{min}=0.6$ T for 28 GHz, the optimum B_{ext} may be higher than 1.8 T. Therefore, we decided to construct the same type of ion source as RIKEN 28 GHz SC-ECRIS because the existing ion source could provide a high enough magnetic field for production of both Ca^{16+} and V^{13+} ion beams. In addition, as each ion source could provide the same condition, we could easily apply the results from one ion source to the other ion source. Figure 8 shows a photograph of the ion source installed on the platform of the ion source room. The ion beam produced with the ion source was injected into the radio frequency quadrupole (RFQ) linac installed in the next room through the LEBT.

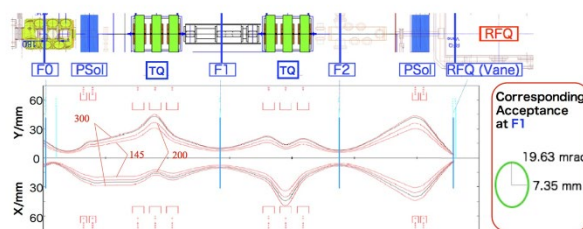


Figure 9: Schematic drawing of the LEBT (upper) and calculated results of beam trajectories (lower).

The detailed structure of the LEBT and its first results are described in ref. [18]. The LEBT consists of several quadrupole magnets, diagnostics systems, and focusing solenoid coils, as shown in Fig. 9. The lower figure shows the calculated trajectories of the ion beam, which had emittances of 145, 200, and 300 π mm*mrاد. The average of four root mean square emittances of the V^{13+} ion beam was ~ 200 π mm*mrاد in the test experiments. It was assumed that most of the produced beam was transported in the LEBT. Furthermore, for safe operation of the intense beam in the long-term, it was important to minimize beam loss

in the accelerators. Therefore, we install the emittance slits (Fig. 10, left) at the beam focus point (F1 in Fig. 9), which shape the beam in the phase spaces ($x-x'$ and $y-y'$), as shown in the light figure of Fig. 10.

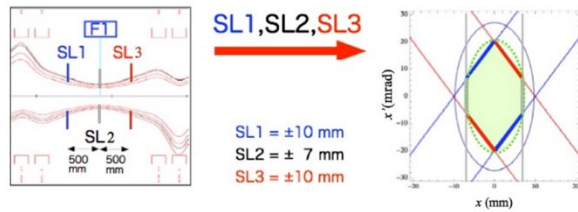


Figure 10: Schematic drawing of the emittance slits (left) and the shape of the emittance cut-off with slits (right).

In July 2018, we extracted the first beam from the ion source. The beam intensity of Ar^{11+} was $90 \mu\text{A}$ at an extraction voltage of 15 kV and an injected microwave power of 600 W. From this autumn, 28 GHz microwaves will be injected into the ion source to further increase beam intensity.

CONCLUSIONS

We systematically studied the effect of the magnetic mirror ratio on beam intensity of various charge state heavy ions with 18 and 28 GHz microwaves. The beam intensity was saturated at $B_{\text{inj}}=1.6-2.0B_{\text{ext}}$ and $B_r=1-1.2B_{\text{ext}}$, which was similar to operation of the high B mode. The optimum B_{ext} to maximize beam intensity depended on the charge state of the heavy ion. It was qualitatively reproduced by the scaling law. We produced an intense V^{13+} ion beam based on our systematic study, and we obtained $400 \text{ e}\mu\text{A}$ of the V^{13+} ion beam with a microwave power of $\sim 2 \text{ kW}$ and a B_{ext} of 1.4 T. For long-term operation, we produced $100-200 \text{ e}\mu\text{A}$ of V^{13+} ions with the new HTO. We used

these results to construct the new ECRIS with the same structure as the existing SC-ECRIS and LEBT. In July 2018, we successfully extracted $90 \mu\text{A}$ of Ar^{11+} ions from the new ECRIS at a microwave power (18 GHz) of 600 W.

REFERENCES

- [1] K. Morita, *Proceedings of the 14th International Symposium on Nuclei in the Cosmos (NIC2016)*, JPS Conf. Proc. 14, 010004, 2017.
- [2] O. Kamigaito et al., *Proceedings of IPAC2016*, Busan, Korea, TUPMR022.
- [3] Y. Yano, *Nucl. Instrum. Methods B261*, 1009, 2007.
- [4] R. Geller, *Electron Cyclotron Resonance Ion Sources and ECR Plasmas*, Institute of Physics, Bristol, 1996, and references therein.
- [5] R. Geller et al., *Proc. 8th Int. Conference on ECR Ion Sources and Their Applications*, NSCL report MSUCP-47, MSU, Dec. 1987, p.1.
- [6] T. Antaya and S. Gammino, *Rev. Sci. Instrum.* 65, 1723, 1998.
- [7] S. Gammino et al., *Rev. Sci. Instrum.* 67, 4109, 1996.
- [8] D. Hitz et al., *Rev. Sci. Instrum.* 73, 509, 2002.
- [9] T. Kurita et al., *Nucl. Instr. and Meth. B* 192, 429, 2002.
- [10] Y. Higurashi et al., *Rev. Sci. Instrum.* 85, 02A953, 2014.
- [11] G. D. Alton and D. N. Smithe, *Rev. Sci. Instrum.* 65, 775, 1994.
- [12] K. Golovanivsky, *Instrum. Exp. Tech.* 28, 989, 1986.
- [13] R. Post, *The course and workshop on Phys. of mirrors*, Vienna, Italy, 1987.
- [14] N. Itagaki, et al., *J. Plasma Fusion Res. SERIES*, 4 305, 2001.
- [15] J. Ohnishi et al., to be published in *Proc. of ECRIS2018*, Catania, Italy, 10-14 Sep 2018.
- [16] J. Ohnishi et al., *Rev. Sci. Instrum.* 87, 02A709, 2015.
- [17] Z.Q. Xie, and C.M. Lyneis, *Rev. Sci. Instrum.* 66, 4218, 1995.
- [18] T. Nagatomo et al, to be published in *Proc. of ECRIS2018*, Catania, Italy, 10-14 Sep 2018.